

Mounting Configuration Factor for Building Integrated Photovoltaic and Retrofitted Grid-connected Photovoltaic System

*Noor Farhana Yusoff, Nor Zaini Zakaria, Hedzlin Zainuddin, Sulaiman Shaari

Abstract— This paper presents the findings of a study to determine the effects of immediate built environment (mounting configuration) on output generated by photovoltaic (PV) module for building integrated photovoltaic (BIPV) and retrofitted PV systems under Malaysian climate. All the systems under study are grid-connected PV (GCPV) system. Eight GCPV systems used in this study; four for BIPV systems and the other four for retrofitted systems. Data for PV module temperature, ambient temperature, plane-of-array solar irradiance and AC power were logged at 5-min interval for all systems. The operating temperature were analysed as the temperature differential with respect to the ambient temperature. The mounting factor was established for both mounting configuration type.

Index Terms—PV modules; retrofitted system; BIPV systems; mounting configuration factors; metal roof

I. INTRODUCTION

Photovoltaic (PV) is a technology that converts light energy directly into electrical energy. The electrical output generated by the PV modules depends on several factors and the factors can be categorised into three groups; heat effect, light input and other factors. Basically heat effect is due to the type of mounting configuration and the air gap under the PV array, while light input is due to the intensity of the solar irradiance (G) and shading at the site. Dirt accumulates on the PV surface and aging are under other factors.

There are three common mounting configuration type in Malaysia; free-standing, retrofitted and building integrated photovoltaic (BIPV) system. Free-standing system is considered as the best type since it has greater air flow beneath the PV array. Retrofitted mounting is referring to the installation of PV modules on top of the existing roof tiles with suitable brackets to hold the PV modules. The small air gap between the module and the roof surface can limit the air flow through it. The main concern for this type of installation is the heat build-up underneath the PV array since the air gap is limited. In addition to the limited ventilation, the temperature of the roofing material can also directly affect the operating temperature of the PV modules. BIPV is a condition where PV modules become part of the building such as roof, atrium and parking lot. Depending on application, BIPV system might has same problem as retrofitted due to limited ventilation. Since

Malaysia experience high and uniform temperature, ambient environmental condition can have a profound effect on the overall performance of the system.

PV module temperature (T_{cell}) is one of the main factor that has directly effect on electrical output generation [1]. Therefore, several studies have been done to quantify the temperature of PV modules. The modelling of T_{cell} can be divided into two categories; analytical and empirical modelling. Analytical modelling is a study based on theoretical formula while empirical modelling based on experimental measured data. Many empirical studies [1]–[9] have considered only ambient environmental factors which is refers to ambient temperature (T_{amb}), solar radiation level (G), wind speed (w_s), relative humidity (RH) and wind direction when predicting temperature of PV modules.

Some studies have make relation between the immediate built environments of the installation on the temperature of the PV module. The immediate built environment refers to the type of roof material and the spacing between the roof surface and the PV modules.

Study by Zakaria et al. (2013) found that the T_{cell} and temperature difference (ΔT) is dependent on the type of roofing material, PV technology, solar irradiance and the air gap height in between PV module and roof surfaces [10]. Zakaria et al. (2014) extended their study to further investigate the thermal impact on the cell temperature of crystalline silicon photovoltaic (PV) modules in Malaysian climate and the findings were consistent with their previous study [11]. Recently, Ye et al. (2013) gave a comprehensive review on influencing factors of operating PV module temperature mounted on rooftops which are metal and concrete roof [12]. Their study focused on temperature rise above ambient over heat flux [9] and in order to decrease the PV module temperature guidelines for module installation established.

Skoplaki et al. (2008) introduces a dimensionless mounting parameter, ω , for various PV array mounting situation [13] when predicting temperature of PV modules and electrical output.

Table 1. Mounting Coefficient

Mounting type	ω
Free-standing	1.0
Flat roof	1.2
Sloped roof	1.8 (1.0-2.7)
Façade roof	2.4 (2.2-2.6)

However, all the above mentioned studies required many factors to calculate T_{cell} , which are limited to be

obtained; a simple expression would be useful for quick application. A simple linear expression that relates T_{amb} , T_{cell} and temperature difference ΔT is used in this study is [14]:

$$T_{cell} = T_{amb} + \Delta T \quad (1)$$

In addition, all existing studies worked on the relationship between module temperature and the ambient, or built environment only. However, there exist only a few studies that related to power output of PV modules under load with the ambient environmental factors in equatorial climate countries.

The present study is motivated by the need to take into consideration the impact of immediate built environment when predicting the temperature of PV module because this will affect the sizing and prediction of PV system performance and also on economics. Therefore, this paper attempts to provide a more details investigations regarding the effects of mounting configurations.

II. METHODOLOGY

The PV systems under Sustainable Energy Development Authority (SEDA) Malaysia monitoring are all grid-connected PV (GCPV) system. A broad variety of locations around Malaysia with different system sizes and mounting configuration has been selected, with the aim of making sample of representative as possible.

Further information of about these system can be found in Tables 2 and 3. In this study, only system greater or equal than 72 kW but less or equal than 425 kW were chosen and under SEDA categories of capacity for installation the range is referring to Part 3. For retrofitted system, all the PV array were mounted on metal roof. The PV modules used for all systems in this study were polycrystalline technology.

Eight GCPV systems were used in this study; four for BIPV systems and the other four for retrofitted system.

B3_01; B refers to type of mounting configuration which is BIPV, 3 refers to categories of installation capacity which is Part 3, and 01 refers to number of system.

Data for PV module temperature, ambient air temperature, plane-of-array solar irradiance and AC power were logged at 5-min interval for all systems.

Table 2. System Specification

System	Capacity (kW)	Inclination	Mounting configuration	Duration of data (days)
B3_01	132	5°	BIPV	7
B3_02	425	5°	BIPV	7
B3_03	340	10°	BIPV	8
B3_04	425	10°	BIPV	7
R3_01	180	5°	Retrofitted	7
R3_02	425	5°	Retrofitted	7
R3_03	425	5°	Retrofitted	6
R3_04	180	5°	Retrofitted	7

Table 3. Categories for Capacity Installation Under SEDA Malaysia [15]

Categories	Installation capacity
Part 1	≤ 12 kW
Part 2	> 12 kW but < 72 kW
Part 3	≥ 72 kW but ≤ 425 kW
Part 4	> 425 kW

III. RESULTS AND DISCUSSION

A. Irradiance profile

Figure 1 to Figure 8 are depicted the daily irradiance profile for all systems under study. As illustrated in Figure 1 to Figure 8, all systems recorded the occurrence of G more than 1000 Wm^{-2} except for system B3_01. Table 4 presents the summary of maximum irradiance (G_{max}), average irradiance (G_{avg}) and average Peak Sun Hour (PSH) for all systems. Highest recorded PSH is 5.505 h for R3_03 while the lowest is 4.214 h for R3_01. In this study, the data were filtered and only G greater than 0 Wm^{-2} selected.

Table 4. Average and Maximum Value of Solar Irradiance and Peak Sun Hour

Syste m	G_{max} (Wm^{-2})	G_{avg} (Wm^{-2})	Average PSH (h)
B3_01	989	444.03	5.408
B3_02	1127	362.29	4.378
B3_03	1091	448.94	5.432
B3_04	1089	481.95	5.359
R3_01	1176	378.16	4.214
R3_02	1158	416.92	4.780
R3_03	1172	427.32	5.015
R3_04	1106	463.33	5.505

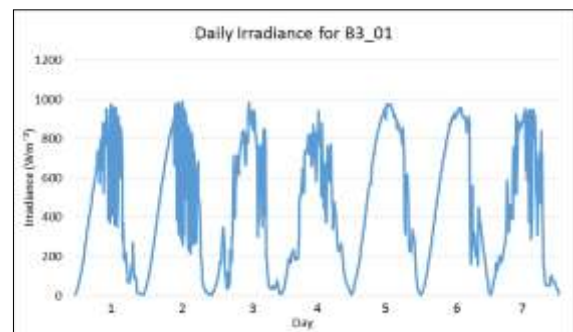


Fig. 1. Daily irradiance profile for B3_01

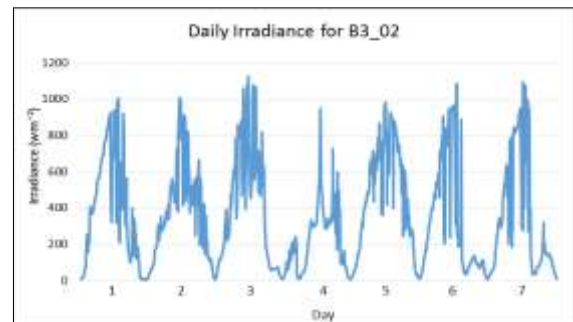


Fig. 2. Daily irradiance profile for B3_02

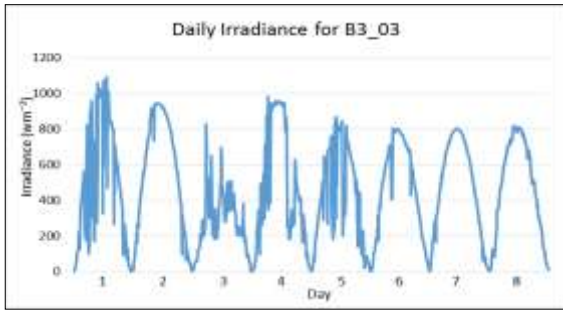


Fig. 3. Daily irradiance profile for System B3_03

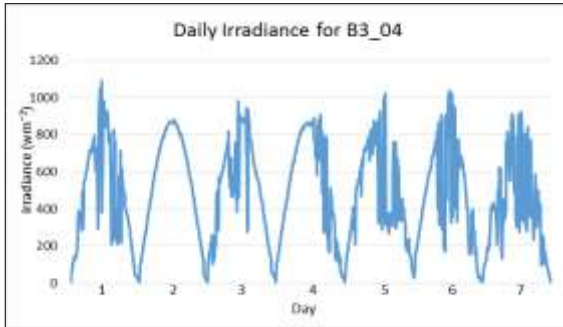


Fig. 4. Daily irradiance profile for System B3_04

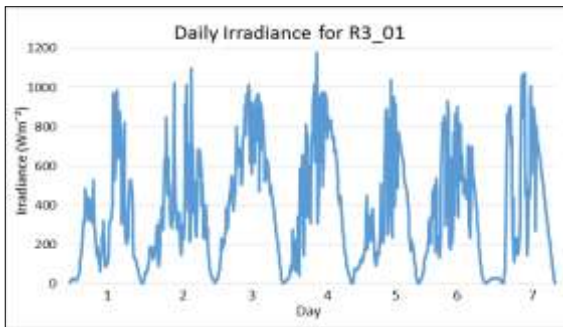


Fig. 5. Daily irradiance profile for System R3_01

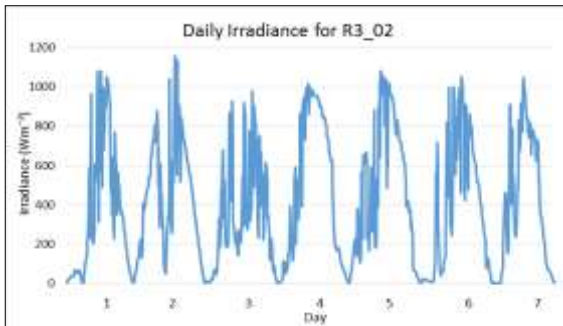


Fig. 6. Daily irradiance profile for System R3_02

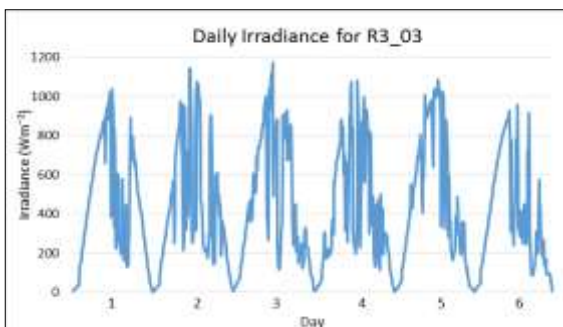


Fig. 7. Daily irradiance profile for System R3_03

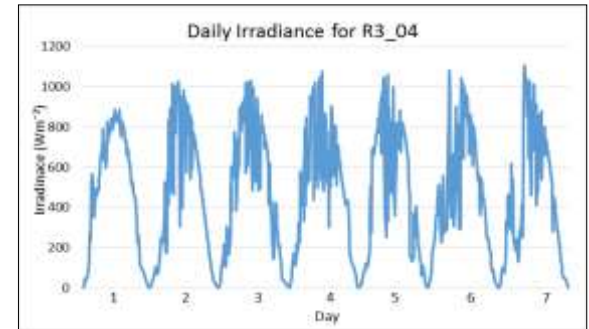


Fig. 8. Daily irradiance profile for System R3_04

B. Temperature Difference

The temperature difference, ΔT , was calculated using the following formula:

$$\Delta T = T_{cell} - T_{amb} \tag{2}$$

The results for all systems are summarized in Tables 5 and 6. The findings are as follows:

- ΔT generally increases with G.
- For BIPV systems, ΔT for B3_01 has similar pattern B3_03, while B3_02 has similar pattern with B3_04. And ΔT for B3_01 and B3_03 are higher than B3_02 and B3_04. The ΔT ranges from 4.667 °C to 28.894 °C.
- While for retrofitted systems, all systems show similar pattern with ΔT ranges from 6.929 °C to 24.390 °C.
- Retrofitted system are expected to have higher ΔT due to limited air ventilation beneath PV array but the results show that two BIPV system has higher ΔT compared to retrofitted system.

Table 5. Average Temperature Difference for BIPV System

Bins (±50 Wm ²)	Temperature Difference (ΔT) (°C)			
	B3_01	B3_02	B3_03	B3_04
200	6.804	4.667	6.000	5.307
400	15.619	9.374	11.298	10.710
600	19.598	13.759	17.667	15.585
800	25.552	16.671	26.783	18.359
1000	28.894	18.824	25.923	18.609

Table 6. Average Temperature Difference for Retrofitted System

Bins (±50 Wm ²)	Temperature Difference (ΔT) (°C)			
	R3_01	R3_02	R3_03	R3_04
200	7.357	6.929	7.331	8.057
400	12.081	10.658	11.730	14.895
600	16.379	15.122	15.345	16.158
800	19.154	18.608	20.783	18.779
1000	21.792	20.897	24.390	22.732

Regression for P_{ac_exp} and P_{ac_mea} vs ΔT

Expected AC power (P_{ac_exp}) was calculated using Equation 3 and compared with the measured AC power (P_{ac_mea}) by plotting in the same scatter plot graph against ΔT . Regression analysis was used to analyse the graph.

$$P_{ac_exp} = P_{mp_stc} \times f_g \times f_{p_tem} \times f_{age} \times f_{dirt} \times f_{mm} \times \eta_{inv} \times \eta_{pv_inv} \quad (3)$$

Referring to Figure 9 to Figure 16, it shows that all the graphs increase in linear manner with gradient varies from 2.8712 to 14.452 and R² ranges from 0.5477 to 0.8822. R² ranges from 0 to 1 for perfect fit. The gradient varies from 2.8712 to 14.452 due to different of system capacity.

For BIPV systems, the regression line for P_{ac_mea} is above the regression line P_{ac_exp} except for B3_03 (Figure 11), where the regression line of P_{ac_mea} crossed with P_{ac_exp}. Based on B3_03 graph, at ΔT ≈ 10 °C, P_{ac_exp} seems to be under predicted.

For retrofitted systems, the regression line for P_{ac_mea} generally below the regression line of P_{ac_exp} except for R3_03 (Fig. 15).

Factor of mounting configuration, f_m can be defined as ratio of average P_{ac_mea} to P_{ac_exp} in order to eliminate the effect of capacity and the results were tabulated in Table 5. The f_m for BIPV system is higher than the retrofitted system due to different thermal impact experience by different mounting type. Based on calculation, the f_m obtained for different mounting types were:

- BIPV ; f_m = 1.0467
- Retrofitted; f_m = 0.9613

This normalized mounting factor (with respect to the P_{ac_mea}) can now be used to modify Equation 3. Thus, the modified AC expected power, P_{ac_exp_corr} is given by:

$$P_{ac_exp_corr} = P_{mp_stc} \times f_g \times f_{p_tem} \times f_{age} \times f_{dirt} \times f_{mm} \times \eta_{inv} \times \eta_{pv_inv} \times f_m \quad (4)$$

P_{ac_exp_corr} was calculated and plotted in the same graph with P_{ac_mea} and P_{ac_exp} to compare the regression line. Figure 9 shows that, the regression line for P_{ac_exp_corr} most likely overlapping with P_{ac_mea}.

Table 7. Mounting Configuration Factor

System	Average Pac_mea (kW)	Average Pac_exp (kW)	Pac_mea / Pac_exp	Mounting configuration factor (f _m)
B3_01	48.083	46.665	1.0304	1.0467
B3_02	137.968	129.580	1.0647	
B3_03	123.074	119.048	1.0338	
B3_04	183.402	173.369	1.0579	
R3_01	52.129	55.838	0.9336	0.9613
R3_02	136.695	143.812	0.9505	
R3_03	144.088	146.642	0.9826	
R3_04	67.157	68.608	0.9783	

Fig. 9. Expected AC power and measured AC power versus temperature difference (ΔT) for B3_01

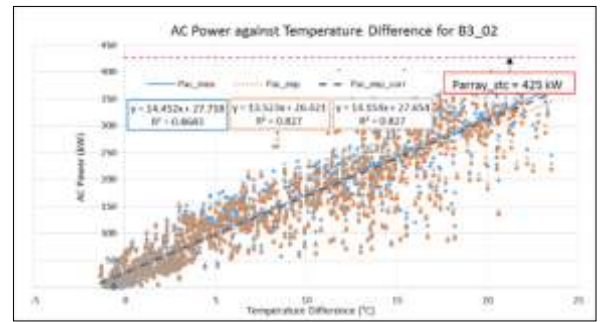


Fig. 10. Expected AC power and measured AC power versus temperature difference (ΔT) for B3_02

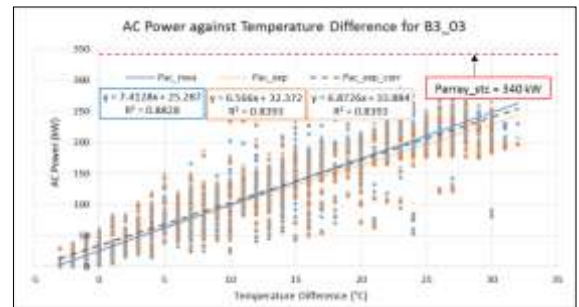


Fig. 11. Expected AC power and measured AC power versus temperature difference (ΔT) for B3_03

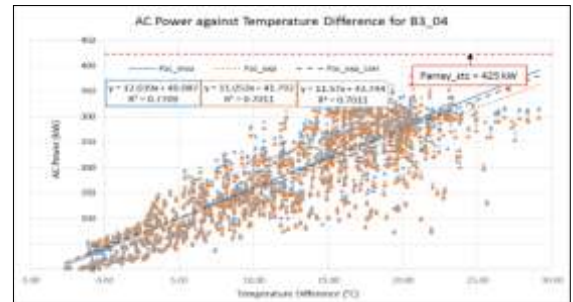


Fig. 12. Expected AC power and measured AC power versus temperature difference (ΔT) for B3_04

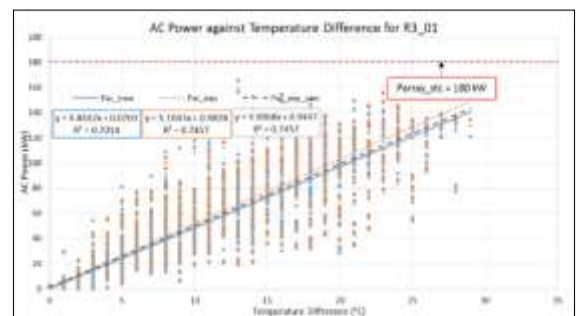
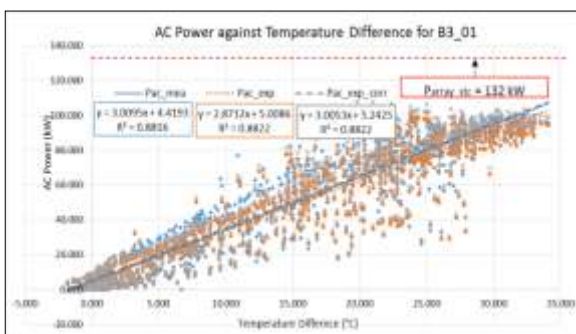


Fig. 13. Expected AC power and measured AC power versus temperature difference (ΔT) for R3_01



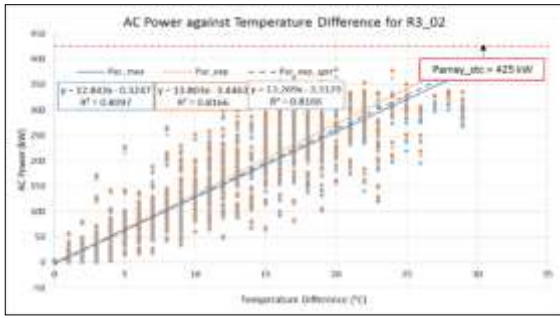


Fig. 14. Expected AC power and measured AC power versus temperature difference (ΔT) for R3_02

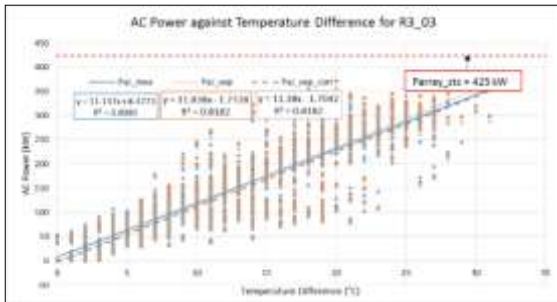


Fig. 15. Expected AC power and measured AC power versus temperature difference (ΔT) for R3_03

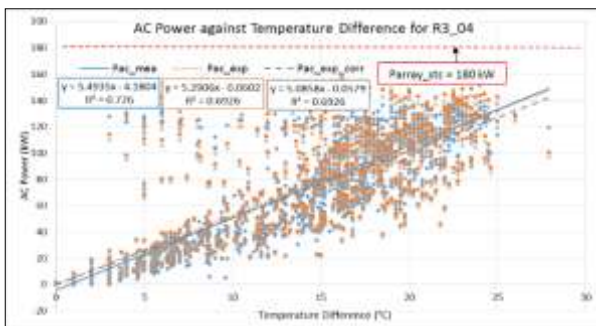


Fig. 16. Expected AC power and measured AC power versus temperature difference (ΔT) for R3_04

C. Specific Yield (SY)

Specific yield was calculated by using Equation 4. Table 8 shows the summary of daily specific yield for each system. In this regard, the BIPV system is expected to produce higher SY compared to retrofitted system because of greater air flow. However, it is depending on the application of BIPV.

$$SY = \frac{Y_f}{P_{array_stc}} \quad (4)$$

Table 8. Daily Specific Yield

System	Daily Average SY (kWh/kW _p)
B3_01	4.695
B3_02	3.993
B3_03	4.474
B3_04	4.354
R3_01	3.621
R3_02	4.103
R3_03	4.216
R3_04	4.505

IV. CONCLUSION

In this study, the aim was to determine the effect of immediate built environment (mounting configuration) on output generated by the PV module. Some important observations are noted and summarize below:

- ΔT for BIPV systems ranges from 4.667 °C to 28.894 °C while for retrofitted systems it ranges from 6.929 °C to 24.390 °C.
- Mounting configuration factor for BIPV, f_m is 1.0467
- Mounting configuration factor for retrofitted, f_m is 0.9613

This findings enhance our understanding that effect of mounting configuration should be addressed properly because this will reduce the power production of PV system and then will cause lost in income.

This research has thrown up many questions in need for further investigation since these findings were based on non-simultaneous data due to the constraints of the study. Further work needs to be done to estimate the percentage of power reduction under control environment thus will help making the findings more reliable and acceptable.

ACKNOWLEDGMENT

The authors wish to express gratitude to Ministry of Higher Education Malaysia and Universiti Teknologi MARA for the support for providing financial support under research grant of FRGS/2/2014/TK06/UITM/02/5; in particular to Assoc Professor Dr Ahmad Malik Omar, Head of Research Centre (GERC) and Dr Shahril Irwan Sulaiman for sharing the data for this study.

REFERENCES

- [1] P. Trinuruk, C. Sorapipatana, and D. Chenvidhya, "Estimating operating cell temperature of BIPV modules in Thailand," *Renew. Energy*, vol. 34, no. 11, pp. 2515–2523, 2009.
- [2] H. Zainuddin, "Module Temperature Modelling for Free-standing Photovoltaic System in Equatorial Climate," Universiti Teknologi MARA, 2014.
- [3] "Modelling of operating temperature for thin film modules for free-standing systems in Malaysia," *Clean Energy and Technology (CEAT), 2013 IEEE Conference on*. pp. 455–460, 2013.
- [4] M. Koehl, M. Heck, S. Wiesmeier, and J. Wirth, "Modeling of the nominal operating cell temperature based on outdoor weathering," *Sol. Energy Mater. Sol. Cells*, vol. 95, no. 7, pp. 1638–1646, 2011.
- [5] E. Skoplaki and J. a. Palyvos, "On the temperature dependence of photovoltaic module electrical performance: A review of efficiency/power correlations," *Sol. Energy*, vol. 83, no. 5, pp. 614–624, 2009.
- [6] A. M. Muzathik, "Photovoltaic Modules Operating Temperature Estimation Using a Simple Correlation," vol. 4, pp. 151–158, 2014.
- [7] A. Q. Jakhriani, A. K. Othman, A. R. H. Rigit, and S. R. Samo, "Determination and comparison of different photovoltaic module temperature models for Kuching, Sarawak," *2011 IEEE 1st Conf. Clean Energy Technol. CET 2011*, pp. 231–236, 2011.
- [8] IEC 61215, "Crystalline Silicon Terrestrial Photovoltaic (PV) Modules - Design Qualification and Type Approval," 2005.
- [9] R. G. Ross Jr, "Interface design considerations for terrestrial solar cell modules," in *12th Photovoltaic Specialists Conference*, 1976, vol. 1, pp. 801–806.
- [10] N. Z. Zakaria, H. Zainuddin, S. Shaari, S. I. Sulaiman, and R.

